Australian Government

Department of Defence

Defence Science and
Technology Organisation

Wavelet Decomposition for Discrete Probability Maps

Emily Brown, Samuel Picton Drake & Anthony Finn

Electronic Warfare and Radar Division

Defence Science and Technology Organisation

DSTO–TN–0760

ABSTRACT

Modern day electronic warfare often contains a heterogeneous mix of distributed sensors. This mix of sensors provides information about the probability of emitters being located at certain points. This discrete probability map (DPM) must be reported to the commander or some other decision maker in a timely fashion.

This report shows that with respect to current methods the most effective way to transmit the DPM is through wavelet decomposition. Following an introduction into wavelet theory we go on to discuss the specifics of the Haar wavelet. Using a sample image, we show how to decompose data by wavelets, specify a compression ratio, transmit a specific region of interest only and reconstruct the data from the wavelets. Having established these techniques we give a specific example of a DPM generated by noisy sensors trying to locate a radar from time difference of arrival, bearings and scan-rate measurements. We conclude the report with a discussion of wavelet basis functions other than the Haar wavelets.

APPROVED FOR PUBLIC RELEASE

APPROVED FOR PUBLIC RELEASE

Wavelet Decomposition for Discrete Probability Maps

EXECUTIVE SUMMARY

In the context of distributed electronic warfare, which is often a complex environment with many emitters and different types of receivers, discrete probability maps (DPM) can be the only accurate and effective way to quantify the probability that targets are located at particular points on a grid map. However, depending on the size and resolution of the grid, it may not be possible to disseminate all of this information in a timely manner.

A wavelet decomposition of the DPM allows the receiver to determine what fidelity of information they require and even in what specific region of space they require it. This ability to select the fidelity and region of interest makes the wavelet decomposition a powerful tool in a band limited dynamic environment.

This report shows how to decompose DPMs into wavelets, specify a compression ratio, zoom in on regions of interest, and reconstruct the DPM from its wavelets. While the report concentrates on Haar wavelets, the same principle applies to other families of wavelets whose properties are summarised.

Authors

Emily Brown
Maritime Operations Division

Emily Brown obtained her Bachelor of Applied Science majoring in Mathematical and Computer Modelling in 2006 from the University of South Australia, Mawson Lakes. Part of this degree was undertaken at the University of Twente in The Netherlands. After completing this degree she participated in the Defence Science and Technology Organisation's (DSTO) student vacation program in the Electronic Warfare and Radar Division; before joining the Torpedo Systems Group in the Maritime Operations Division at the DSTO.

___

Samuel Picton Drake
Electronic Warfare and Radar Division

Sam Drake is a senior research scientist in the Defence Science and Technology Organisation (DSTO). He obtained his honours degree in physics from the University of Melbourne, and went on to do a PhD in mathematical physics (General Relativity) at the University of Adelaide. Following a post-doctoral position at the University of Padua, Italy, he joined the Navigation Systems group of DSTO in 1999 working on the operational analysis of the global positioning system (GPS). Since starting at DSTO Sam has worked on a variety of projects ranging from GPS to communication networks. Sam is currently working on autonomous unmanned aerial vehicles (UAVs). Sam is also an adjunct associate lecturer at the University of Adelaide.

___

Anthony Finn
Electronic Warfare and Radar Division

Dr Anthony Finn is Head of DSTO's Automation of the Battlespace Initiative, with broad responsibility for the coordination and leadership of a team of about fifty scientists and engineers across nine DSTO divisions, industry, and academia. He has previously held the positions of Head, Navigation Systems and Head, Strategic & Land EW. Dr Finn has a First Class Honours degree in Engineering and a PhD from Cambridge University. Before moving joining DSTO in 1991 he worked as a research consultant for a number of organisations in Europe. Dr Finn has published around 75 journal and research papers.

Contents

Figures

Tables

1   Introduction

Wavelets are mathematical transformations used to represent a function or signal contained in a finite domain. Wavelets are localised in both frequency and time, which makes many functions and operators using them *sparse* when transformed. This sparse coding makes wavelets a useful tool in data compression.

There are many families of wavelets, but this report will begin by examining one of the simplest, the Haar wavelet. The Haar wavelet is the first known wavelet developed in the early 1900's by Alfred Haar [6]. The Haar wavelet transform allows data to be encoded in levels of detail. An everyday example of this can been seen on Netscape's World Wide Web, when an image is called from a URL address, the image appears in installments, beginning with a crude approximation and gradually adding detail until the final complete image is displayed. This is called *progressive image transmission* and may be useful if the receiver can decide on an early approximation of the image that they do not want to see the whole image and can stop the process and move onto to something else; or if the connection is lost, an approximation of the image has been sent, so not all the information has been lost. The approximations of the image can also be stored using a lot less space than the original data.

2   Wavelets

Wavelets have received much attention as they have been developed due to the fact that they are useful at representing diverse classes of functions sparsely. This implies that they can represent many functions with far fewer coefficients than the alternative of a Fourier or polynomial basis [12]. The Discrete Wavelet Transform (DWT) technique is becoming preferred over the Discrete Cosine Transform (DCT) as in the DWT the entire image is transformed and compressed as a single data object rather than block by block, as with the DCT [7]. This allows for a uniform distribution of compression errors across the entire image. Examples of functions for which wavelets perform better than other techniques are those which have sharp jumps or discontinuities [6], such as images where the intensity may undergo sharp changes across an edge boundary.

A wavelet transform maps a signal $f(x)$ into a two-dimensional function of $a > 0$ and $\tau \in \mathbb{R}$, where a is the scale (it scales a function by compressing or stretching it) and τ is the translation.

In order for the wavelet transform to be well-defined, we restrict ourselves to square integrable functions, $f(x) \in \mathcal{L}^2(\mathbb{R})$, meaning that

$$\int f^2(x)\, dx < \infty \tag{1}$$

A function $\psi(x)$ is known as a (Mother) wavelet if $\mathcal{L}'(\mathbb{R})$.

The continuous wavelet transform $\Psi(a, \tau)$ of signal $f(x)$ is given by:

$$\Psi(a, \tau) = \frac{1}{\sqrt{a}} \int f(x)\, \psi\left(\frac{x - \tau}{a}\right)\, dx \tag{2}$$

Definition of a wavelet:

1. Admissibility, $\psi(x) \in \mathcal{L}^2(\mathbb{R})$ such that

$$\int_{\mathbb{R}} \frac{|\hat{\psi}(\omega)|^2}{|\omega|} d\omega < \infty \tag{3}$$

2. Regularity, $\psi(x)$ decreases rapidly[1]

Condition 1. implies that $\hat{\psi}(0) = 0 \Rightarrow \int_{\mathbb{R}} \psi(t)dt = 0$
Condition 2. implies that ψ has some concentration in both space and frequency.

2.1 Derivation

An image can be reduced to a piecewise-constant function on the half open interval $[0, 1)$. For each nonnegative integer j, let $\mathcal{V}^j$ be the vector space of piecewise constant functions on $[0, 1)$, with constant pieces over each of the 2^j equal subintervals. So every one-dimensional image with 2^j pixels is a vector in $\mathcal{V}^j$. [17]
If an image is represented by a given function $f(x)$, with a resolution level of j, where the function $f_j(x)$ approximates $f(x)$.

$$f_j(x) = \sum_i c_i^j \phi_i^j(x) \qquad \text{See Section 2.2} \tag{4}$$

The function can be approximated at the next resolution level $j + 1$ by:

$$f_{j+1}(x) = f_j(x) + d_j(x) \tag{5}$$

where $d_j(x)$ are considered to be the details of the image.
We now need to define a basis for each vector space $\mathcal{V}^j$. We will call the basis functions for the space $\mathcal{V}^j$, *scaling functions*, which shall be denoted by $\phi(x)$.
Such that $\cup_{j \in (Z)} \mathcal{V}^j = \mathcal{L}^2(\mathbb{R})$ and $\cap_{j \in (Z)} \mathcal{V}^j = \phi$

$$\phi_i^j(x) = 2^{j/2} \phi(2^j x - i) \tag{6}$$

The closed subspaces $\{\mathcal{V}^j\}$ of $\mathcal{L}^2(\mathbb{R})$ form a nested sequence that provides successively better approximation to $\mathcal{L}^2(\mathbb{R})$, the space of square integrable functions; know as a multiresolution analysis of $\mathcal{L}^2(\mathbb{R})$.

$$\mathcal{V}^0 \subset \mathcal{V}^1 \subset \mathcal{V}^2 \subset \ldots \tag{7}$$

---

[1]Often a wavelet is further improved with the condition that ψ and its derivatives up to $r \in l^\infty(\mathbb{R})$ decrease rapidly and $\int_{\mathbb{R}} x^q \psi(n)dn = 0$ for $0 \le q \le r$. This improves a certain amount of regularity and localisation of f.

Therefore any function from subspace $\mathcal{V}^0$ can be represented with basis functions from $\mathcal{V}^1$, and any function from $\mathcal{V}^1$ can be represented with basis functions from $\mathcal{V}^2$, and so on.

It is necessary to choose an inner product defined on the vector space $\mathcal{V}^j$. In this case we will choose the standard inner product,

$$\langle f|g \rangle = \int_0^1 f(x)\,g(x)\,dx \qquad \text{for } f,\ g \in \mathcal{V}^j \tag{8}$$

Now we can define a new vector space $\mathcal{W}^j$ as the orthogonal complement of $\mathcal{V}^j$ in $\mathcal{V}^{j+1}$, ie $\mathcal{V}^{j+1} = \mathcal{V}^j \oplus \mathcal{W}^j$. The wavelets in $\mathcal{W}^j$ are a way of representing the parts of a function in $\mathcal{V}^{j+1}$ that cannot be represented in $\mathcal{V}^j$.

A collection of linearly independent functions $\psi_i^j(x)$ spanning $\mathcal{W}^j$ are called wavelets. These basis functions have two important properties: [19]

1. The basis functions ψ_i^j of $\mathcal{W}^j$, together with the basis functions ϕ_i^j of $\mathcal{V}^j$ form a basis for $\mathcal{V}^{j+1}$.

2. Every basis function ψ_i^j of $\mathcal{W}^j$ is orthogonal to every basis function ϕ_i^j of $\mathcal{V}^j$ under the chosen inner product.

2.2   Discrete Wavelet Transform

Given an input function $f(x) \in L^2(\mathbb{R})$ which is only known to a resolution level of j. An approximation of the function $f(x)$ on level j can be described by $f_j(x)$

$$f_j(x) = \sum_i c_i^j \phi_i^j(x) \tag{9}$$

Where

$$\sum_i c_i^j\,\phi_i^j = \sum_i c_i^{j-1}\phi_i^{j-1} + \sum_i d_i^{j-1}\psi_i^{j-1} \tag{10}$$

$$= \sum_i^{j-2} c_i^{j-2}\phi_i^{j-2} + \sum_i^{j-2} d_i^{j-2}\psi_i^{j-2} + \sum_i^{j-2} d_i^{j-1}\psi_i^{j-1} \tag{11}$$

$$\vdots$$

Because ϕ_i^j

$$\mathcal{V}^j = \mathcal{V}^{j-1} \oplus \mathcal{W}^{j-1} \tag{12}$$

Giving

$$f(x) = c_0^0\,\phi_0^0 + d_0^0\,\psi_0^0 + \sum_{i=0}^1 d_i^1\,\psi_i^1(x) + \sum_{i=0}^2 d_i^2\,\psi_i^2(x) + \ldots + \sum_{i=0}^{j-1} d_i^{j-1}\,\phi_i^{j-1}(x) \tag{13}$$

Where $\phi_i^j(x)$ is the scaling function defined in section 2.1 and the coefficients c_i^j are given by

$$\text{Scaling coefficient:} \qquad c_i^j = \int f_j(x)\phi_i^j(x)dx \tag{14}$$

And the coefficients d_i^j are given by

$$\text{Wavelet coefficient:} \qquad d_i^j = \int f_j(x)\psi_i^j(x)dx \qquad (15)$$

ψ^j and ϕ^i are orthogonal so that, if $i \neq j$

$$\int \psi_k^j \, \phi_l^i \, dx = 0 \qquad (16)$$

3   The Haar Wavelet

The simplest wavelet is the Haar wavelet and can be defined on $[0, 1)$, by:

$$\psi_i^j(x) = 2^{j/2}\psi(2^j x - i), \qquad i = 0, ..., 2^j - 1 \qquad (17)$$

where

$$\psi(x) = \begin{cases} 1 & \text{for} \quad 0 \leq x < \frac{1}{2} \\ -1 & \text{for} \quad \frac{1}{2} \leq x < 1 \\ 0 & \text{otherwise} \end{cases} \qquad (18)$$

The scaling functions can be represented by

$$\phi_i^j(x) = 2^{j/2}\phi(2^j x - i) \qquad i = 0, ..., 2^j - 1 \qquad (19)$$

where

$$\phi(x) = \begin{cases} 1 & \text{for} \quad 0 \leq x < 1 \\ 0 & \text{otherwise} \end{cases} \qquad (20)$$

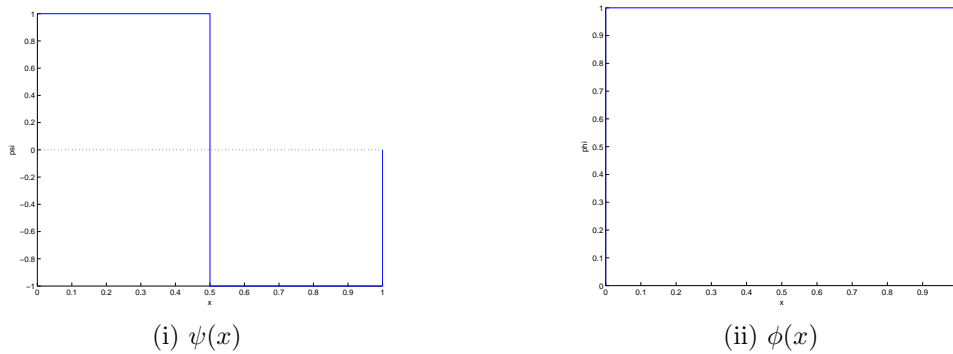(i) $\psi(x)$ (ii) $\phi(x)$

Figure 1: $\psi(x)$ and $\phi(x)$

3.1   Haar Wavelet Transform

To demonstrate how the Haar wavelet transform is implemented, let us consider a string of numbers, which will represent a one-dimensional image. (The numbers have been chosen so that fractions are avoided for simplicity).

$$\begin{bmatrix} 8 & 10 & 6 & 4 \end{bmatrix} \tag{21}$$

The wavelet transform is an averaging and differencing process. Consider the pairs of pixels (8, 10) and (6, 4), take the average of each pair, 9 and 5, and then record this in the next line. Then record the difference of the averages from the first value of the pair (marked in bold). This process is then applied to this new string resulting in the final line, where the differences are just carried down. As follows:

$$\begin{bmatrix} 8 & 10 & 6 & 4 \end{bmatrix} \tag{22}$$
$$\begin{bmatrix} 9 & 5 & \textbf{-1} & \textbf{1} \end{bmatrix} \tag{23}$$
$$\begin{bmatrix} 7 & \textbf{2} & \textbf{-1} & \textbf{1} \end{bmatrix} \tag{24}$$

The differences recorded to the righthand side are known as the *detail coefficients*. The first number in the final string is the *overall average*. The recursive process of averaging and differencing is called a *filter bank*.

By doing this process no information has been lost nor new information gained. The original image can be reconstructed by recursively adding and subtracting the detail coefficients from the lower resolution versions.

Note that the string contains four values, 2^2, which means that the averaging and differencing process is done in two steps. If the string contained eight values 2^3, then the process would be done in three steps, and so on.

An advantage of transforming an image into this new string is that many of the detail coefficients are considerably small in magnitude. Truncating or removing these smaller coefficients gives a much sparser string which can be stored more compactly. However, by truncating the detail coefficients, information has been lost and the original image cannot be fully restored. This is lossy image compression.

Select a non-negative threshold value ϵ, if any of the detail coefficients are less than or equal to ϵ, set them to zero. If $\epsilon = 0$, this gives lossless compression, and we can reconstruct the original image. If $\epsilon > 0$, this gives lossy compression, only an approximation of the image can be reconstructed.

3.2   Function Representation

Using the scaling functions and wavelet functions previously defined in Section 2.
The example can again be calculated.

The original image: $f(x)$ $\begin{bmatrix} 8 & 10 & 6 & 4 \end{bmatrix}$

$$f(x) = c_0^2\,\phi_0^2(x) + c_1^2\,\phi_1^2(x) + c_2^2\,\phi_2^2(x) + c_3^2\,\phi_3^2(x) \qquad \begin{bmatrix} 8 & 10 & 6 & 4 \end{bmatrix} \qquad (25)$$

$$f(x) = c_0^1\,\phi_0^1(x) + c_1^1\,\phi_1^1(x) + d_0^1\,\psi_0^1(x) + d_1^1\,\psi_1^1(x) \qquad \begin{bmatrix} 9 & 5 & -1 & 1 \end{bmatrix} \qquad (26)$$

$$f(x) = c_0^0\,\phi_0^0(x) + d_0^0\,\psi_0^0(x) + d_0^1\,\psi_0^1(x) + d_1^1\,\psi_1^1(x) \qquad \begin{bmatrix} 7 & 2 & -1 & 1 \end{bmatrix} \qquad (27)$$

The progressive addition of detail in equation (27) is shown in Figure 4.

The coefficients c and d are the values calculated in Section 3.1 is displayed to the right.
In equation (27) $\phi_0^0(x)$ represents the overall average, $\psi_0^0(x)$ the broad detail and $\psi_0^1(x)$ and $\psi_1^1(x)$ are the two types of finer detail possible in a function in $\mathcal{V}^2$.
The Haar basis for $\mathcal{V}^j$ with $j > 2$ includes these functions as well as narrower translations of the wavelets $\psi(x)$.

| (i) $\phi_0^2(x)$ | (ii) $\phi_1^2(x)$ | (iii) $\phi_2^2(x)$ | (iv) $\phi_3^2(x)$ |

| (v) $\phi_0^1(x)$ | (vi) $\phi_1^1(x)$ |
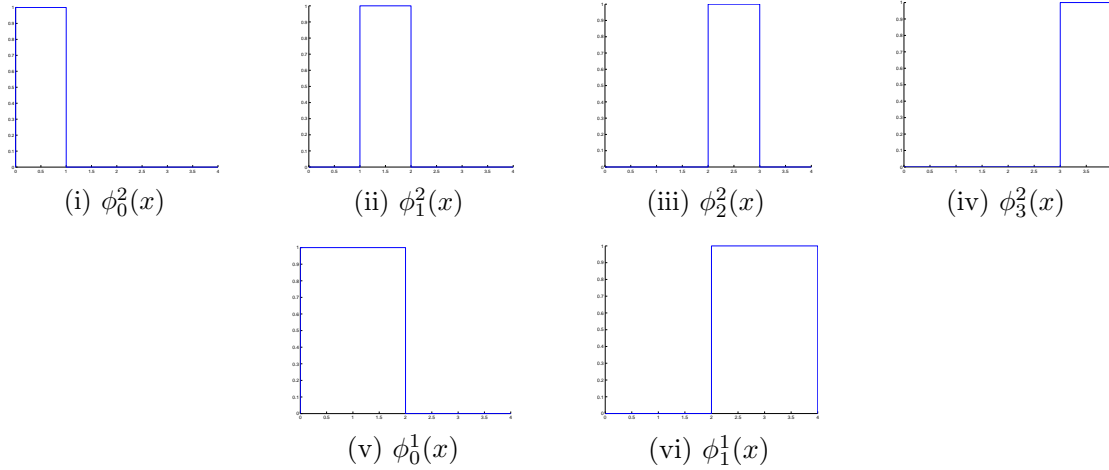
Figure 2: *The bases of $\mathcal{V}^2$ (ϕ_i^2) and $\mathcal{V}^1$ (ϕ_i^1)*

| (i) $\psi_0^1(x)$ | (ii) $\psi_1^1(x)$ | (iii) $\psi_0^0(x)$ |

Figure 3: *The Haar wavelets for $\mathcal{W}^1$ (ψ_i^1) and $\mathcal{W}^0$ (ψ_i^0)*

Figure 4: *Adding detail to $f(x)$ resulting in equation (27)*

4 Orthonormal Basis

4.1 Orthogonality

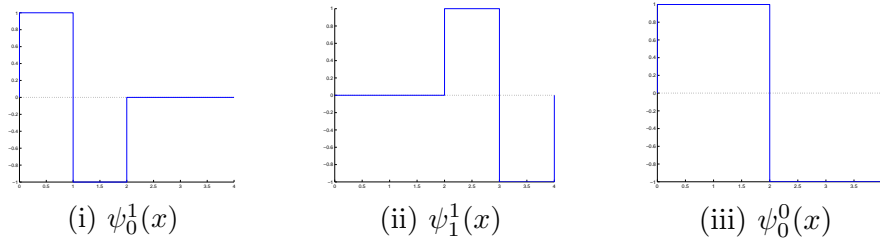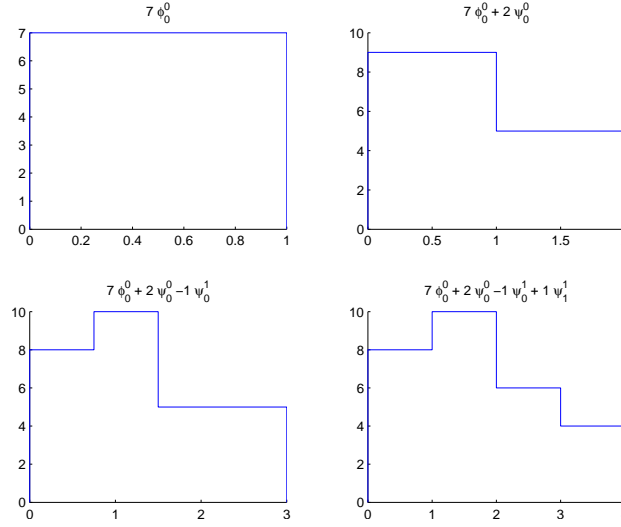An orthogonal basis is one where all the basis functions are orthogonal to one another with respect to the standard norm. For the Haar basis ϕ_0^0, ψ_0^0, ψ_0^1, ψ_1^1, ... are all orthogonal to each other.

4.2 Normalisation

It is known that a basis function $u(x)$ is normalised if $\langle u|u \rangle = 1$
The Haar basis is normalised by the inclusion of the constant factor $2^{j/2}$ in the wavelet and scaling functions.

$$\phi_i^j(x) \quad = \quad 2^{j/2}\,\phi(2^j x - i) \tag{28}$$

$$\psi_i^j(x) \quad = \quad 2^{j/2}\,\psi(2^j x - i) \tag{29}$$

The constant factor $2^{j/2}$ is chosen to ensure $\langle u|u \rangle = 1$ for the standard inner product. Implemented in the averaging and differencing process of Section 3.1, each set of pairs to be averaged is divided by $\sqrt{2}$ instead of 2.

$$\text{e.g.} \qquad \frac{a+b}{\sqrt{2}} \quad \text{used instead of} \quad \frac{a+b}{2}$$

This gives an *orthonormal* basis, one which is both orthogonal and normalised.

7

5   Image Compression

The image that will be used in this example is a greyscale jpeg 256×256 image, downloaded from the internet [5]. Matlab code from Mulcahy [10] has been implemented to perform the Haar wavelet transform and display the images. The image AnneFrank.jpg is read into Matlab using /`imread` and stored as an image data array. The image of Anne Frank (Figure 5) is represented by a 256×256 array of numbers, ranging from 1, which represents black to 256, which represents white (different scales can be used). As 256 or 2^8 different shades of gray are used, the image is described as an 8-bit image.

Figure 5: *Original Image: Anne Frank*

Let us just consider a small section of the image around Anne Frank's eye to demonstrate the process being applied to the whole image.

$$
A = \begin{bmatrix}
30 & 25 & 27 & 31 & 33 & 30 & 28 & 32 \\
26 & 25 & 26 & 27 & 27 & 25 & 30 & 47 \\
21 & 30 & 27 & 25 & 24 & 27 & 47 & 86 \\
29 & 31 & 28 & 25 & 27 & 39 & 74 & 131 \\
29 & 30 & 24 & 26 & 37 & 67 & 118 & 169 \\
49 & 42 & 39 & 51 & 82 & 123 & 166 & 188 \\
67 & 63 & 63 & 81 & 119 & 159 & 187 & 188 \\
73 & 75 & 74 & 87 & 108 & 127 & 141 & 143
\end{bmatrix}
$$

To transform this image matrix, we need to perform the averaging and differencing process described in section 3.1. The first row yields:

$$
\begin{bmatrix}
30 & 25 & 27 & 31 & 33 & 30 & 28 & 32 \\
38.89 & 41.01 & 44.55 & 42.43 & \mathbf{-8.89} & \mathbf{-14.01} & \mathbf{-11.55} & \mathbf{-14.43} \\
56.50 & 61.50 & \mathbf{-17.61} & \mathbf{-16.95} & \mathbf{-8.89} & \mathbf{-14.01} & \mathbf{-11.55} & \mathbf{-14.43} \\
83.44 & \mathbf{-26.94} & \mathbf{-17.61} & \mathbf{-16.95} & \mathbf{-8.89} & \mathbf{-14.01} & \mathbf{-11.55} & \mathbf{-14.43}
\end{bmatrix}
$$

The row operations above can be described by:

$$
\begin{array}{llll}
\text{row 1} & A[1,:] & : & \mathcal{V}^3 & (30) \\
\text{row 2} & A[2,:] & : & \mathcal{V}^2 \otimes \mathcal{W}^2 & (31) \\
\text{row 3} & A[3,:] & : & \mathcal{V}^1 \otimes \mathcal{W}^1 \otimes \mathcal{W}^2 & (32) \\
\text{row 4} & A[4,:] & : & \mathcal{V}^0 \otimes \mathcal{W}^0 \otimes \mathcal{W}^1 \otimes \mathcal{W}^2 & (33)
\end{array}
$$

This process is applied to all the rows in matrix A, resulting in the partially transformed matrix:

$$
\mathcal{F}(A) =
\begin{bmatrix}
83.44 & -26.94 & -17.61 & -16.95 & -8.89 & -14.01 & -11.55 & -14.43 \\
82.38 & -30.38 & -15.94 & -27.73 & -10.06 & -11.48 & -9.77 & -24.45 \\
101.47 & -49.97 & -15.44 & -55.94 & -15.06 & -9.77 & -12.06 & -47.05 \\
135.76 & -79.26 & -14.07 & -88.83 & -13.43 & -9.48 & -19.67 & -70.96 \\
176.78 & -122.28 & -12.78 & -121.96 & -12.72 & -11.36 & -36.54 & -84.94 \\
258.80 & -172.30 & -27.81 & -134.54 & -17.69 & -24.64 & -62.96 & -84.32 \\
327.74 & -190.74 & -45.08 & -129.92 & -24.92 & -38.82 & -77.58 & -78.17 \\
292.74 & -138.24 & -49.85 & -93.33 & -31.65 & -39.84 & -58.17 & -59.82
\end{bmatrix}
$$

This matrix is then transposed and the averaging and differencing process repeated to the new rows, and then transformed back, to give the fully transformed matrix $T = \mathcal{F}(\mathcal{F}(A)^T)$:

$$
T =
\begin{bmatrix}
516.88 & -190.38 & -2.83 & -127.46 & 0.75 & -11.25 & -35.00 & -48.25 \\
-231.88 & 121.88 & 3.18 & 41.54 & -3.25 & 11.25 & 30.00 & -10.25 \\
-35.71 & 36.06 & -2.75 & 49.75 & 6.01 & -3.54 & 7.07 & 26.52 \\
-91.04 & -12.55 & 9.25 & -46.50 & 1.41 & 6.01 & -4.24 & -24.75 \\
0.75 & 3.75 & -0.35 & 9.90 & 2.00 & -1.50 & 0.50 & 6.50 \\
-24.25 & 19.25 & -2.83 & 20.15 & -3.50 & -0.50 & 4.50 & 9.00 \\
-60.00 & 24.00 & 2.83 & -12.02 & -4.00 & 5.00 & 5.50 & -14.50 \\
24.75 & -42.25 & -0.35 & -16.97 & 3.00 & -2.50 & -10.50 & 0.50
\end{bmatrix}
$$

The transformed matrix T has one overall average in the top left hand corner, and the remaining values are detail elements. This new transformed matrix has many values which are smaller in magnitude than any of the elements in A, these values represent areas where a value has similar adjacent elements.

From here the decision can be made by choice of the threshold value whether the process will be lossless compression or lossy compression. If a threshold value $\epsilon = 0$ is chosen then the original image A can be reconstructed, by simply reversing the process. However if a threshold value $\epsilon > 0$ is chosen, such as $\epsilon = 10$, all elements less than or equal to 10 are set to 0 in T, to produce the doctored matrix D:

$$D = \begin{bmatrix} 516.88 & -190.38 & 0 & -127.46 & 0 & -11.25 & -35.00 & -48.25 \\ -231.88 & 121.88 & 0 & 41.54 & 0 & 11.25 & 30.00 & -10.25 \\ -35.71 & 36.06 & 0 & 49.75 & 0 & 0 & 0 & 26.52 \\ -91.04 & -12.55 & 0 & -46.50 & 0 & 0 & 0 & -24.75 \\ 0 & 0 & 0 & 0 & 0 & 0 & 0 & 0 \\ -24.25 & 19.25 & 0 & 20.15 & 0 & 0 & 0 & 0 \\ -60.00 & 24.00 & 0 & -12.02 & 0 & 0 & 0 & -14.50 \\ 24.75 & -42.25 & 0 & -16.97 & 0 & 0 & -10.50 & 0 \end{bmatrix}$$

This matrix is considerably sparse. Sparse matrices can have properties which make calculating their inverse much less computationally intensive. The inverse wavelet transform is applied to D, which gives the reconstructed matrix R. This process applied to the whole 256×256 matrix of Anne Frank gives the following output (Figure 6).
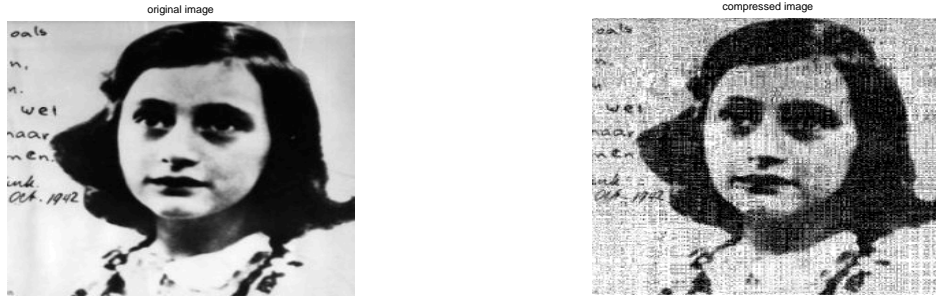

(i) The original image

(ii) The reconstructed image, $\epsilon = 10$

Figure 6: *The original image and the reconstructed image, with threshold $\epsilon = 10$*

Figure 5 contains 65536 nonzero values, hence there are no zero values in the original matrix A. The reconstructed matrix R, with threshold $\epsilon = 10$, contains 33259 nonzero values, and therefore is 50.7492% dense. Or has a compression ratio of 1.9705 to 1.

We can change the threshold value ϵ to examine the quality of the reconstructed image (Figure 7).
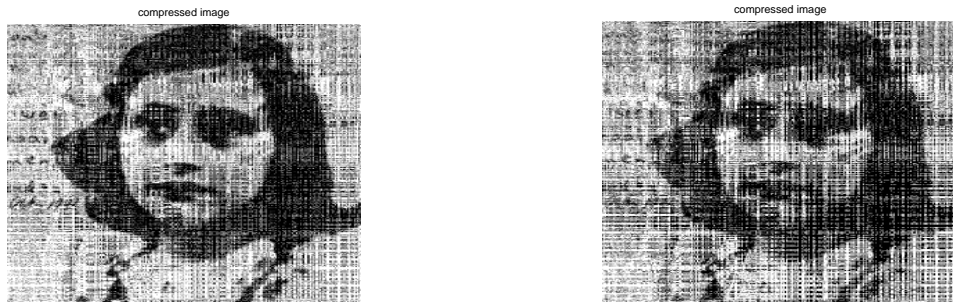
(i) Threshold $\epsilon = 15$ gives a compression ratio of 2.9052 to 1, and the matrix is 34.4208% dense

(ii) Threshold $\epsilon = 20$ gives a compression ratio of 4.2156 to 1, and the matrix is 23.7213% dense

Figure 7: *Reconstructed images*

5.1 Linear Algebra Wavelet Transform

The process of averaging and differencing used to perform the Haar wavelet transform can be done computationally simpler using matrix multiplication. The Haar wavelet transform of the first row of A (from section 5) can be done by the matrix multiplication of the three matrices B_1, B_2 and B_3. [10]

$$B_1 = \begin{pmatrix} \frac{1}{\sqrt{2}} & 0 & 0 & 0 & \frac{1}{\sqrt{2}} & 0 & 0 & 0 \\ \frac{1}{\sqrt{2}} & 0 & 0 & 0 & -\frac{1}{\sqrt{2}} & 0 & 0 & 0 \\ 0 & \frac{1}{\sqrt{2}} & 0 & 0 & 0 & \frac{1}{\sqrt{2}} & 0 & 0 \\ 0 & \frac{1}{\sqrt{2}} & 0 & 0 & 0 & -\frac{1}{\sqrt{2}} & 0 & 0 \\ 0 & 0 & \frac{1}{\sqrt{2}} & 0 & 0 & 0 & \frac{1}{\sqrt{2}} & 0 \\ 0 & 0 & \frac{1}{\sqrt{2}} & 0 & 0 & 0 & -\frac{1}{\sqrt{2}} & 0 \\ 0 & 0 & 0 & \frac{1}{\sqrt{2}} & 0 & 0 & 0 & \frac{1}{\sqrt{2}} \\ 0 & 0 & 0 & \frac{1}{\sqrt{2}} & 0 & 0 & 0 & -\frac{1}{\sqrt{2}} \end{pmatrix}$$

$$B_2 = \begin{pmatrix} \frac{1}{\sqrt{2}} & 0 & \frac{1}{\sqrt{2}} & 0 & 0 & 0 & 0 & 0 \\ \frac{1}{\sqrt{2}} & 0 & -\frac{1}{\sqrt{2}} & 0 & 0 & 0 & 0 & 0 \\ 0 & \frac{1}{\sqrt{2}} & 0 & \frac{1}{\sqrt{2}} & 0 & 0 & 0 & 0 \\ 0 & \frac{1}{\sqrt{2}} & 0 & -\frac{1}{\sqrt{2}} & 0 & 0 & 0 & 0 \\ 0 & 0 & 0 & 0 & 1 & 0 & 0 & 0 \\ 0 & 0 & 0 & 0 & 0 & 1 & 0 & 0 \\ 0 & 0 & 0 & 0 & 0 & 0 & 1 & 0 \\ 0 & 0 & 0 & 0 & 0 & 0 & 0 & 1 \end{pmatrix} \qquad B_3 = \begin{pmatrix} \frac{1}{\sqrt{2}} & \frac{1}{\sqrt{2}} & 0 & 0 & 0 & 0 & 0 & 0 \\ \frac{1}{\sqrt{2}} & -\frac{1}{\sqrt{2}} & 0 & 0 & 0 & 0 & 0 & 0 \\ 0 & 0 & 1 & 0 & 0 & 0 & 0 & 0 \\ 0 & 0 & 0 & 1 & 0 & 0 & 0 & 0 \\ 0 & 0 & 0 & 0 & 1 & 0 & 0 & 0 \\ 0 & 0 & 0 & 0 & 0 & 1 & 0 & 0 \\ 0 & 0 & 0 & 0 & 0 & 0 & 1 & 0 \\ 0 & 0 & 0 & 0 & 0 & 0 & 0 & 1 \end{pmatrix}$$

Where $W = B_1 \, B_2 \, B_3$ and

$$\begin{aligned} \mathcal{L}(A[1, :]) &= \begin{pmatrix} 29.5 & -1.25 & -0.75 & 0.75 & 2.5 & -2 & 1.5 & -2 \end{pmatrix} \\ &= \begin{pmatrix} 30 & 25 & 27 & 31 & 33 & 30 & 28 & 32 \end{pmatrix} W \end{aligned}$$

The columns of the B_i's are orthogonal to each other with respect to the standard inner product, so that implies that each of these matrices is invertible. Therefore the inverse Haar wavelet transform can also easily be performed by matrix multiplication using $W^{-1} = B_3^{-1} B_2^{-1} B_1^{-1}$.

For a matrix of size $2^n \times 2^n$, B_1, $B_2, \ldots, B_n$ are needed to perform the transform to each vector of length 2^n. To transform the whole image matrix we simply follow the same procedure as before and transform each row but now using the linear algebra approach and then transform each of the resulting columns.

Therefore for A of size $2^n \times 2^n$

$$T = ((AW)^T W)^T = W^T AW \tag{34}$$

and

$$A = (T^T W^{-1})^T W^{-1} = (W^{-1})^T TW^{-1} \tag{35}$$

This technique is used in Mulcahy's [11] Matlab code utilised in Section 5.

6   Selecting an Area of the Image

Consider an image being transmitted using the wavelet transform. First a coarse image is transmitted, but from this approximation you can see a smaller section of the image that you are interested in. Instead of waiting for the whole image to be transmitted, it may be more efficient if after making a decision of the area you are interested in, that only this section of the image is transmitted with greater resolution.

From a coarse approximation of the image displayed in Matlab, an area of interest can be selected using `getrect(fig)`. From this selection of an area a smaller image matrix is defined.
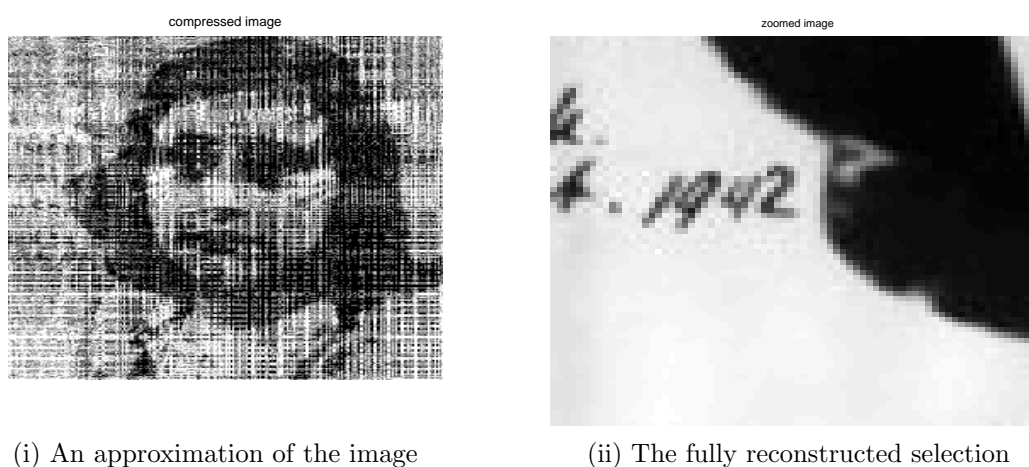

(i) An approximation of the image   (ii) The fully reconstructed selection

Figure 8: Selecting an area of interest from an approximation of the image

Figure 9: The area of interest (full resolution) displayed within coarse image

The rest of the inverse wavelet transform can simply be applied to this new smaller image matrix. It is no longer required to send the rest of the details of the entire image.

6.1   Discrete Probability Maps

A wavelet decomposition of the DPM allows the receiver to determine the detail or resolution of information they require and even a specific section of the image that they require. By following the procedure applied to the image of Anne Frank (Figure 5), the DPM can also be transmitted using the wavelet transform.

Figure 10 is a mesh image of the bivariate probability density function (pdf) from a pair of sensors of three generated targets.
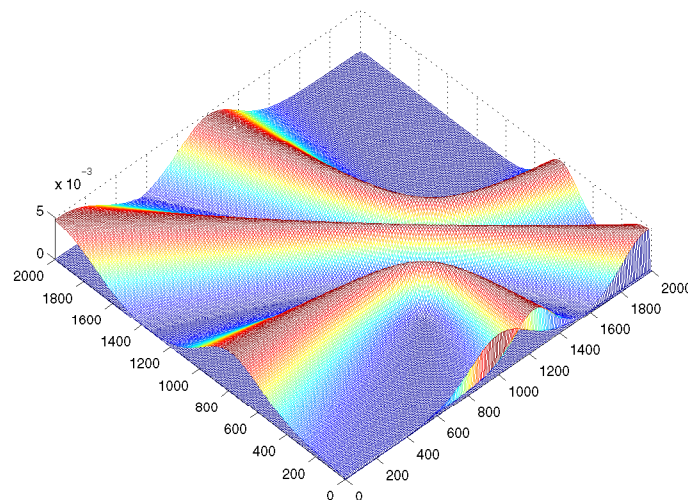

Figure 10: *The pdf from sensor 1 of three generated targets*

From the original image an approximation of the image can be made using the Haar wavelet transform. Again, we can select an area of the image which may be of greater interest and display the finer detail for only this area of the image.
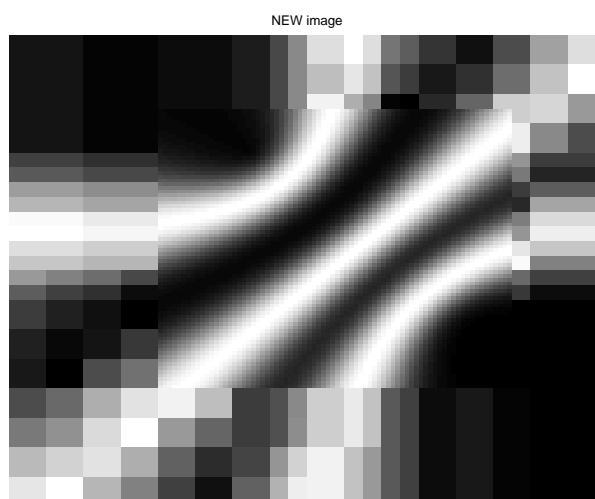

Figure 11: *The area of interest (full resolution) displayed within coarse DPM*

7   Wavelet Families

There are many wavelets available to decompose and analyse both discrete and continuous data. In general a wavelet is any function whose dilations and translations form a Riesz basis [8] for the function space $\mathcal{L}^2(\mathbb{R})$ [10]. There are infinitely many wavelet multiresolution bases for $\mathcal{L}^2(\mathbb{R})$. The different wavelet families make different trade offs between how compactly the basis functions are localised in space and how smooth they are. Within each family of wavelets are wavelet subclasses distinguished by their number of coefficients. The wavelets are classified within a family most often by the number of *vanishing moments* [6].

A wavelet has m vanishing moments if

$$m_l = \int_{-\infty}^{\infty} x^l \psi(x) dx = 0 \qquad \text{for } l = 0, \ldots, m-1 \tag{36}$$

Advantages of these vanishing moments is that smooth parts of functions will have zero wavelet coefficients associated with them [12].

The simplest wavelet is the one previously discussed, the Haar wavelet. The Haar wavelet is the only known wavelet that is compactly supported, orthogonal and symmetric.

In image processing applications, since human vision is more tolerant of symmetric error than an asymmetric one, it is desirable to use symmetric wavelets [14]. Also symmetric wavelets make it easier to deal with the boundaries of an image. All orthogonal wavelets are asymmetric, however Daubechies [3] has shown that with some modifications, it is possible to design orthogonal wavelets that are nearly symmetric.

Note that perfect symmetry is only possible for complex wavelet filters, biorthogonal wavelets, infinite support wavelets and multi-wavelets [14]. For many applications it is preferred to have real filter coefficients, therefore only one choice remains for a symmetric wavelet, the biorthogonal wavelet. For biorthogonal wavelets, there are two scaling functions $\phi(t)$ and $\tilde{\phi}(t)$, and two wavelet functions $\psi(t)$ and $\tilde{\psi}(t)$, therefore in each case there are two wavelet filters associated with each wavelet $\psi(t)$ and $\tilde{\psi}(t)$. The Cohen-Daubechies-Feauveau wavelet (CDF) is the first family of biorthogonal wavelets.

Below is a review of some of the more commonly known wavelets:
Symlets are nearly symmetrical wavelets proposed by Daubechies as modifications to the the Daubechies db family. Properties of the two wavelet families are very similar. The Mexican Hat wavelet has no scaling function and is derived from a function that is proportional to the second derivative function of the Gaussian probability density function. The Morlet wavelet has no scaling function but is explicit/complex. Biorthogonal wavelets use two wavelets, one for decomposition and the other for reconstruction, instead of using the same one.

Table 1: *Wavelet families*

Wavelet	Orthogonal	capable of perfect reconstruction	Symmetric in shape
Haar	✓	✓	
Daubechies (dbN)	✓	✓	
Symlets	✓	✓	nearly symmetric
Coiflets	✓	✓	
Meyer		✓	✓
Morlet			✓
Mexican Hat			✓
Biorthogonal		✓	✓

8   Conclusion and Further Work

Discrete probability maps DMPs are an accurate and effective way of representing the probability of emitters being at certain locations. An alternative approach to sharing the situation is to describe the probability distribution by a sum of gaussians. The advantage of the sums of gaussian's approach, as opposed to DMPs is the situational awareness can be represented by significantly less data. The disadvantage of the sum of gaussians approach is that it can lead to inaccuracy and bias [16].

In this report we have shown how discrete probability maps can be decomposed into wavelets and distributed through a network. We showed how the data is transmitted as a course approximation with increasing fidelity as more and more data arrives. This refining of the data allows the end user to decide when to stop the transmission or send high fidelity data only for a specified region.

Having demonstrated the concept with Haar wavelets we plan to implement it in Distributed Electronic Warfare Situational Awareness and Response (DEWSAR) as a method for sharing situational awareness between UAVs. If this approach is successful we plan to investigate if any improvement can be gained by using other wavelet basis functions, such as those mentioned in Section 7

References

1. P. M. Bentley and J. T. E. McDonnell. Wavelet transforms: an introduction. *Electronics & Communication Engineering Journal*, 6(4):175–186, 1994. 0954-0695.

2. Y.T. Chan. *Wavelet basics.* Kluwer Academic Publishers, Bosten, 1995.

3. Ingrid Daubechies. *Ten Lectures on wavelets.* Society for Industrial and Applied Mathematics, Philadelphia, 1992.

4. R. A. DeVore, B. Jawerth, and B. J. Lucier. Image compression through wavelet transform coding. *Information Theory, IEEE Transactions on*, 38(2):719–746, 1992. 0018-9448.

5. Frank. Anne frank, the hollywood photograph. *wikapedia*, 1942.

6. Amara Graps. An introduction to wavelets. *IEEE Computational Science and Engineering*, 2(2), 1995.

7. S. Grgic, K. Kers, and M. Grgic. Image compression using wavelets. volume 1, pages 99–104 vol.1, 1999.

8. G. Kaiser. *A Friendly Guide to Wavelets.* Birkhuser, Bosten, 1994.

9. Yves Meyer. *Wavelets Algorithms & Applications.* the Society, Philadelphia, 1993.

10. Colm Mulcahy. Plotting and scheming with wavelets. *Mathematics Magazine*, 69(5):323–343, 1996.

11. Colm Mulcahy. Image compression using the haar wavelet transform. *Spelman College Science & Mathematics Journal*, 1(1):22–31, 1997.

12. G. P. Nason. A little introduction to wavelets. pages 1/1–1/6, 1999.

13. William Press, Saul Teukolsky, William Vetterling, and Brian Flannery. Wavelet transforms. In *Numerical Recipes in C: The Art of Scientific Computing*, pages 591–606. Cambridge University Press, New York, 2002.

14. Ali M Reza. Wavelet characteristics, what wavlet should i use? *Spire Lab, UWM*, 1999.

15. O. Rioul and M. Vetterli. Wavelets and signal processing. *Signal Processing Magazine, IEEE*, 8(4):14–38, 1991. 1053-5888.

16. Branko. Ristic, Sanjeev. Arulampalam, and Neil James Gordon. *Beyond the Kalman filter : particle filters for tracking applications.* Artech House, Boston, Mass., 2004.

17. E. J. Stollnitz, A. D. DeRose, and D. H. Salesin. Wavelets for computer graphics: a primer.1. *Computer Graphics and Applications, IEEE*, 15(3):76–84, 1995. 0272-1716.

18. E. J. Stollnitz, T. D. DeRose, and D. H. Salesin. Wavelets for computer graphics: a primer. 2. *Computer Graphics and Applications, IEEE*, 15(4):75–85, 1995. 0272-1716.

19. Eric J. Stollnitz, Tony D. DeRose, and David H. Salesin. *Wavelets for Computer Graphics, Theory and Applications.* Morgan Kaufmann Publishers, San Francisco, 1996.

20. Gilbert Strang. Wavelets. *American Scientist*, 82:250–255, 1994.

21. Brani Vidakovic and Peter Mueller. Wavelets for kids, a tutorial introduction. *http://www2.isye.gatech.edu/ brani/wp/kidsA.ps*, 1994.

22. J. Zhu. Image compression using wavelets and jpeg2000: a tutorial. *Electronics & Communication Engineering Journal*, 14(3):112–121, 2002. 0954-0695.

DEFENCE SCIENCE AND TECHNOLOGY ORGANISATION DOCUMENT CONTROL DATA	1. CAVEAT/PRIVACY MARKING

2. TITLE Wavelet Decomposition for Discrete Probability Maps	3. SECURITY CLASSIFICATION Document (U) Title (U) Abstract (U)

4. AUTHORS Emily Brown, Samuel Picton Drake & Anthony Finn	5. CORPORATE AUTHOR Defence Science and Technology Organisation PO Box 1500 Edinburgh, South Australia 5111, Australia

6a. DSTO NUMBER DSTO–TN–0760	6b. AR NUMBER 013-928	6c. TYPE OF REPORT Technical Note	7. DOCUMENT DATE August, 2007

8. FILE NUMBER 2007/1026545/1	9. TASK NUMBER LRR-04/004	10. SPONSOR ABSI	11. No OF PAGES 17	12. No OF REFS 22

13. URL OF ELECTRONIC VERSION http://www.dsto.defence.gov.au/corporate/ reports/DSTO–TN–0760.pdf	14. RELEASE AUTHORITY Chief, Electronic Warfare and Radar Division

15. SECONDARY RELEASE STATEMENT OF THIS DOCUMENT
Approved For Public Release
OVERSEAS ENQUIRIES OUTSIDE STATED LIMITATIONS SHOULD BE REFERRED THROUGH DOCUMENT EXCHANGE, PO BOX 1500, EDINBURGH, SOUTH AUSTRALIA 5111

16. DELIBERATE ANNOUNCEMENT
No Limitations

17. CITATION IN OTHER DOCUMENTS
No Limitations

18. DSTO RESEARCH LIBRARY THESAURUS
Probability Wavelet Transforms Target Acquisition

19. ABSTRACT

Modern day electronic warfare often contains a heterogeneous mix of distributed sensors. This mix of sensors provides information about the probability of emitters being located at certain points. This discrete probability map (DPM) must be reported to the commander or some other decision maker in a timely fashion.

This report shows that with respect to current methods the most effective way to transmit the DPM is through wavelet decomposition. Following an introduction into wavelet theory we go on to discuss the specifics of the Haar wavelet. Using a sample image, we show how to decompose data by wavelets, specify a compression ratio, transmit a specific region of interest only and reconstruct the data from the wavelets. Having established these techniques we give a specific example of a DPM generated by noisy sensors trying to locate a radar from time difference of arrival, bearings and scan-rate measurements. We conclude the report with a discussion of wavelet basis functions other than the Haar wavelets.